A COMPARATIVE EVALUATION OF HEAT DISSIPATION FACTORS FOR OPEN-RACK AND FLOATING SOLAR PHOTOVOLTAIC INSTALLATIONS

[1]Brendan Willemse, [1]Shaun Nielsen, [1]Johannes Pretorius, [1]Michael Owen, [2]Arnold Rix

[1]Department of Mechanical and Mechatronics Engineering, [2]Department of Electrical and Electronic Engineering, Stellenbosch University Private Bag X1, Matieland, 7602, Stellenbosch, South Africa

E-mail: 22635122@sun.ac.za, 19050089@sun.ac.za, jpp@sun.ac.za, mikeowen@sun.ac.za, rix@sun.ac.za

Abstract:

Estimation of solar photovoltaic (PV) module operating temperature is an important component of accurate PV system simulation and design. Faiman's module temperature model provides a simple method of estimating PV module operating temperature using empirical heat dissipation factors (HDFs) and is widely used in PV simulation. This paper presents HDFs for open-rack and floating solar PV (FPV) configurations based on measurements collected on installations near Stellenbosch, South Africa. The paper allows for direct comparison of the HDFs for these different PV configurations under similar solar and ambient conditions. Differences in the thermal characteristics of the configurations are thus highlighted and potential design factors that influence FPV's heat dissipation are outlined.

Keywords: module temperature; open-rack PV; floating photovoltaic (FPV); Faiman model; heat dissipation factors

1. Introduction

It is well known that photovoltaic (PV) systems are susceptible to efficiency losses when exposed to high module operating temperatures. Various methods have therefore been developed to accurately predict the operating temperatures of PV systems. Faiman's [1] model is commonly used to model the heat dissipation of PV modules by correlating the wind speed, ambient temperature, and plane of array (POA) irradiance to the operating module temperatures. Faiman's model has been shown to be relatively accurate across a wide range of PV technologies and climatic operating conditions [2] and provide comparable accuracy to more complex models [3].

Heat dissipation is a critical factor in PV system performance as it directly impacts the modules' temperature and thus efficiency. Different PV configurations (e.g., ground-mounted open-rack, building-attached or floating) experience unique thermal operating conditions and thus display distinct heat dissipation characteristics. For example, ground-based open-rack systems, typically used for large-scale operations (such as utility-scale or commercial PV installations), facilitates relatively uninhibited airflow around the panels. Natural air currents and wind can thus reach and cool the modules and relatively low module temperatures are expected.

Floating solar PV (FPV) systems are installed on the surface of still water bodies and are an emerging technology that can be used in regions with limited land resources for ground-based open-rack PV installations. FPV systems can also contribute to water security (they reduce the amount of water loss due to evaporation throughout the day [4]) and can be coupled with hydropower systems, reducing the cost of renewable energy generation [5]. In theory, these systems should offer improved heat dissipation due to the proximity to a cool water body and some research has shown that FPV systems can be more efficient than ground-based systems [6]. However, there is limited literature on the thermal behaviour of these water-based systems. A method to specifically determine the heat dissipation factors (HDFs) and cell temperature of FPV systems is presented in [7]. The model shows acceptable correlation to measured values however it has not been extensively validated for FPV technology. Dörenkämper et al. [8] modelled the HDFs of FPV systems to determine the impact of different float designs and climates on the HDFs of FPV.

This paper utilizes the Faiman model to predict the heat dissipation factors (HDFs) for a ground-based open-rack PV and FPV system operating in close proximity (and thus under similar operating conditions), enabling a direct comparison between the thermal behaviour of the two technologies. By analysing the heat dissipation characteristics of FPV configurations, valuable

insight into their respective efficiencies and potential design considerations can be gained.

2. Experimental Setup and Methodology

The test sites are located in the Western Cape province of South Africa, with a straight-line distance of 12.7 km between the two sites (see Fig. 1). The region is characterised by a Mediterranean climate with an average maximum summer temperature of 25℃ and minimum winter temperature of 9℃ [9] and high solar resource, 1 649 kWh/kWp [10].

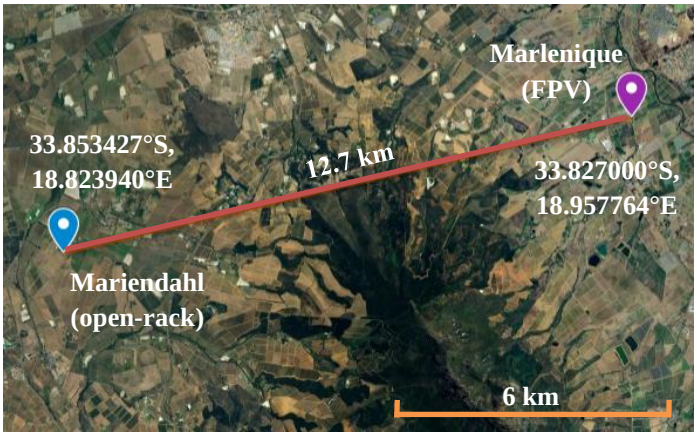

Fig. 1. Geographical map of PV installations

2.1. Open-Rack Installation Details and Data Gathering

The open-rack PV installation monitored in this work is shown in Fig. 2, and located at Mariendahl farm outside Stellenbosch, South Africa. Two PV modules (CS3W-420P) were mounted at a fixed tilt angle of 31°, facing North. The module is rated with an efficiency of 19% and a nominal module operating temperature (NMOT) of 42±3 ℃. The modules were connected in series to a 136 Ω 4 A resistive load, allowing the modules to operate in a closed-circuit condition during the test period.

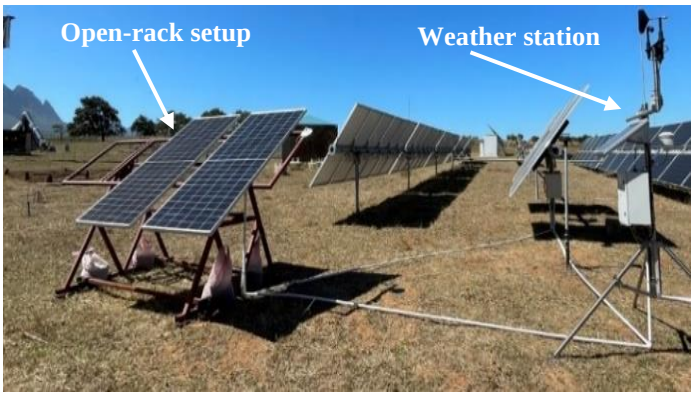

Fig. 2. Mariendahl open-rack system

Two T-type thermocouples were attached to the back side of each module using aluminium tape, positioned at a central and corner cell respectively (similar to Faiman [1]). All module temperature data was logged at one-minute intervals using a Lord TC-Link 200 and recorded using a Lord WSDA Base Station and SensorConnect software. Ambient temperature, wind speed and POA irradiance were collected from a weather station installed near the open-rack structure shown in Fig. 2. Ambient temperature was measured with a shielded HygroVUE5 digital temperature sensor. Wind speed and direction were measured with a R.M. Young 03002 wind sentry and vane. The POA irradiance was measured with a Kipp & Zonen CMP10 pyranometer installed on the open-rack structure, in-plane with the modules.

2.2. FPV Installation Details and Data Gathering

The FPV system is located at Marlenique Estate, Stellenbosch, South Africa (Fig. 3). The PV system consists of 10 x 18 PV modules (CS6U-320P modules) at a fixed tilt angle of 16°. The modules are rated with an efficiency up to 16.97% and a nominal operating temperature (NOCT) of 45±2 ℃. Charge controllers ensure that the modules operate at their maximum power point.

The temperature of the centre module in the Northern row is measured. This module was chosen since its operating environment is likely to be most similar to the open-rack case (limited packing effect in the FPV array), ensuring a comparable assessment to the open-rack experiment.

Fig. 3. Marlenique FPV system

The module and ambient temperatures were measured using a RSPRO PT100 and Campbell Scientific CS109 thermocouple respectively. Two module thermocouples were taped slightly offest from the back face's centre position. The system's equipment was instrumented by the Institute for Energy Technology (IFE) in Norway, therefore the system configuration differs somewhat from the open-rack installation.

Fig. 4. Weather station at FPV installation

The wind speed measurement was taken with a Gill Windsonic wind sensor, while the POA irradiance was measured using a Kipp & Zonen CMP10 pyranometer that is installed in-plane with the PV module tilt angle. The pyranometer and wind speed sensor were both attached to a GeoSun weather station (Fig. 4). The weather station is attached to a mast at the back of the array and stores the data in 1-min intervals. Additionally, the ambient temperature is measured at the centre of the array.

2.3. Data Processing

Thermal models that evaluate the heat dissipation factors for PV modules often assume steady state conditions. Rapid fluctuations in operating conditions therefore degrade the accuracy of the models and filtering is applied to limit the analysis to times of relatively stable conditions. Such filtering is standard practice for thermal measurements on PV modules and an IEC standard [11] has also been developed that describe the measurement and filtering requirements.

For our data, the application of the filtering practice (specifically the filtering of wind) according to the standard resulted in a major reduction in acceptable data points on the open-rack system, and in contrast virtually no difference in the data for the FPV system.

In light hereof, and as our paper determines heat dissipation factors according to the Faiman model, we decided to implement the same filtering strategy as the original paper by Faiman [1]. This strategy does not filter based on wind data, and applies the following:

- Data is stored as 5-min averages.
- Only days with clear sky conditions (i.e. only minor observable irradiance fluctuations) are to be considered.
- Analysis period between 10 am and 2 pm.

For the open-rack installation the module temperature was calculated by averaging the two thermocouple measurements for each module. Out of a potential 92-day testing period between 2023/03/30 and 2023/06/29, data from 29 days with clear skies provided a total of 2330 useable data points.

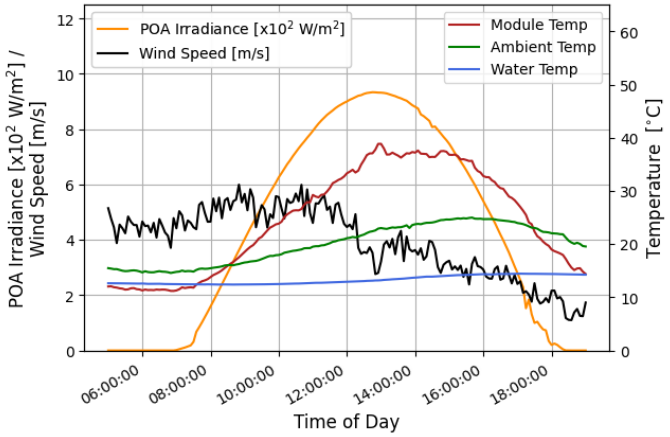

Fig. 5. Unfiltered clear sky data for the FPV site

The GeoSun weather station at the FPV site also reported the average values of the two module thermocouples. During an analysis period of 58 days (2022/08/31-2022/10/28) for the FPV installation, only 13 days had clear sky conditions, resulting in 610 useable data points. The impact of clear sky filtering on the FPV data is illustrated in Fig. 5 (unfiltered) and Fig. 6 (filtered).

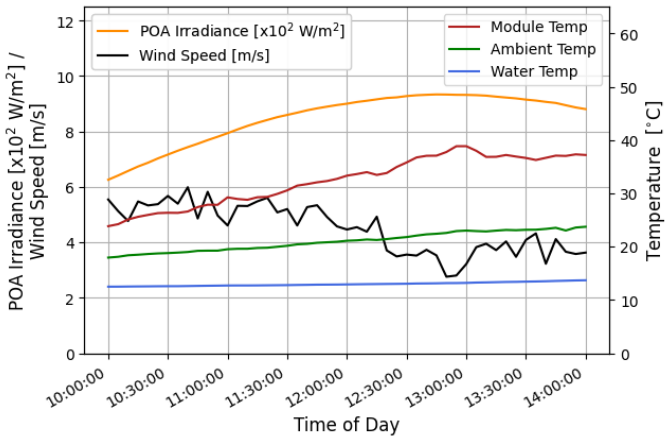

Fig. 6. Filtered clear sky data for the FPV site

2.4. Faiman Module Temperature Model

The thermal model proposed by Faiman [1] utilizes meteorological data as inputs and is based on the Hottel-Whillier-Bliss [12, 13] equation. The modified equation by Faiman decomposes the overall HDF into two components: a constant factor (U_0') and a wind-dependent factor (U_1'). The combined effects of radiation and natural convection heat transfer are represented by U_0', while forced convection heat transfer via wind is represented by U_1'. Faiman relates these parameters to the module and ambient temperatures (T_{mod} and T_{amb}), POA irradiance (H), and wind speed (v_w).

$$\frac{H}{U_0' + U_1' \cdot v_w} = T_{mod} - T_{amb} \quad (1)$$

HDFs are determined from experimental measurements of temperature, POA irradiance and wind speed by linear regression.

3. Results and Discussion

3.1. Environmental Conditions

To evaluate the similarity of the environmental test conditions for the two sites, histograms of the POA irradiance, wind speed and ambient temperatures are presented in Fig. 7 and 8, over the respective test periods. The variables are normalized with respect to the open-rack configuration's maximum values. The open-rack configuration measured values of $H_{max} = 1175.2\ W/m^2$, $v_{w,max} = 6.37\ m/s$, and $T_{amb,max} = 32.8\ ℃$.

The FPV site exhibited higher average wind speeds, whereas the open-rack site consistently encountered a broader range of wind speeds. Both sites maintained similar POA irradiance values throughout the day, with slightly elevated values on average observed at the FPV site. Unlike the open-rack site, the FPV site did not reach the maximum POA irradiance. On average, the FPV site also recorded higher ambient temperatures during the day, although it did not reach the peak temperature observed at the open-rack site. The distribution (negatively skewed) of the ambient temperature for the FPV site can be attributed to the fewer available data points for the analysis period in comparison to the open-rack analysis period. Overall, the disparities in environmental conditions were deemed acceptable for facilitating a direct comparison.

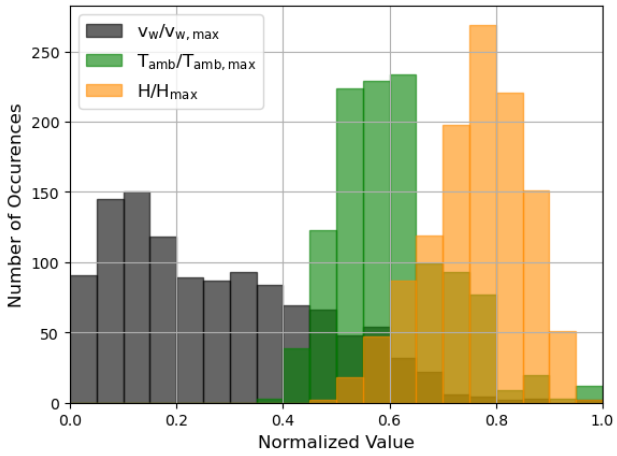

Fig. 7. Open-rack normalised environmental conditions

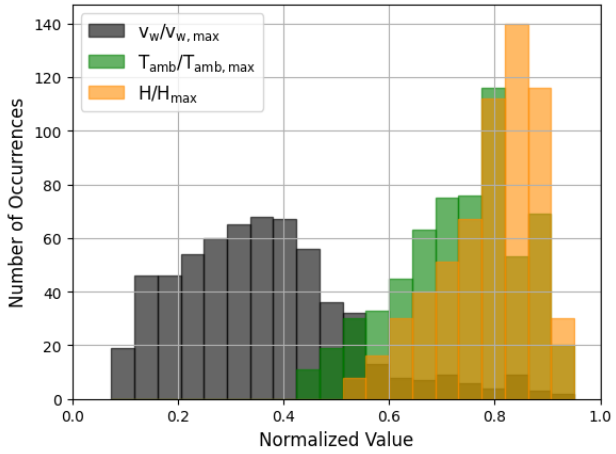

Fig. 8. FPV normalised environmental conditions

3.2. Open-Rack PV Results

The results for the open-rack configuration are shown in Fig. 9. The U_0' and U_1' values ($25.70\ W/m^2K$ and $9.90\ Ws/m^3K$ respectively, with $R^2 = 0.79$) compare well to those initially determined by Faiman [1] ($U_0' = 25\ W/m^2K$, $U_1' = 6.80\ Ws/m^3K$, $R^2 = 0.63$) and open-rack experiments conducted at Stellenbosch University [14] ($U_0' = 26.5\ W/m^2K$ and $U_1' = 5.2\ Ws/m^3K$ at a tilt angle of 23°).

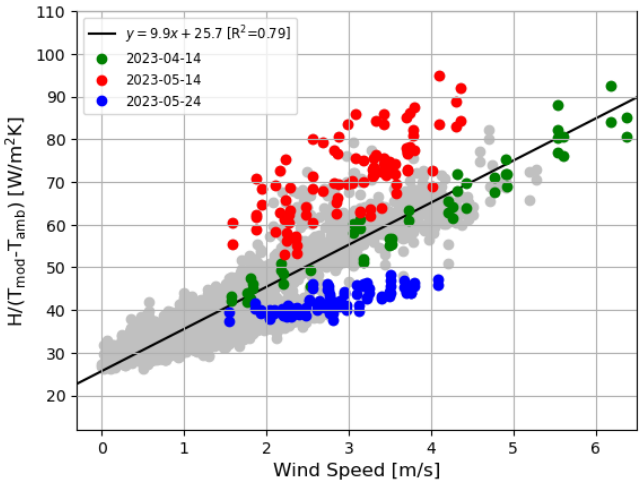

Fig. 9. Open-rack HDF curve

From the 29 clear sky days, data from three different days are highlighted in colour in Fig. 9, and their behaviour and influence on the dataset are examined. In the figure, we observe two outlier days (red and blue) and one trend-aligned day (green) for the open-rack system.

For the day represented by green markers, the increasing trend in HDF aligns with a gradually increasing wind speed (over a large range) throughout the day. Little fluctuation in instantaneous wind speed (limited gusts) during this period

results in little HDF variation around the trendline.

The magnitude of POA irradiance, wind speed and ambient temperature are similar for the days represented by the red and blue data. There is however greater fluctuation in wind speed for the day in red versus the day in blue, causing the respective difference in scatter on the graph. Despite the similar atmospheric conditions, module temperatures for the blue data are higher. As a result, $H/(T_{mod} - T_{amb})$ is lower due to the higher denominator, causing the data points to sit below the trendline. It is our hypothesis that the difference in module temperature between these two days can be ascribed to a difference in wind direction.

A comparison between the measured and predicted (using the HDFs and Eq. 1) module temperatures is shown in Fig. 10. The model predicted the measured temperatures with a root-mean-square error (RMSE) of 2.56 ℃. This compares well with the RMSE of 1.86 ℃ obtained by Faiman [1] and 1.7-2.5 ℃ in [5].

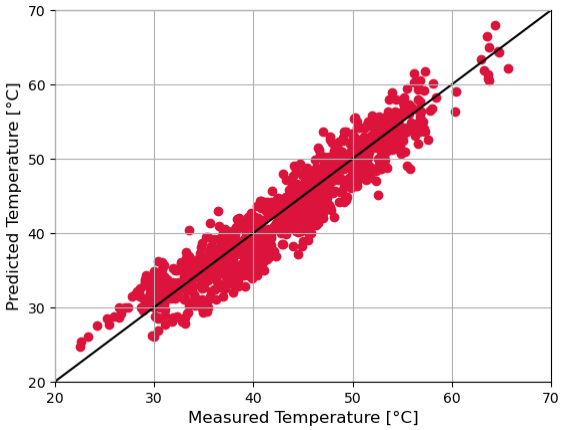

Fig. 105. Open-rack temperature prediction

3.3. FPV Results

Fig. 11 shows the FPV results. The coefficient of determination value of the fitted data is reasonably high (R^2 = 0.73). However, it is worth noting that the FPV analysis had fewer data points available compared to the open-rack experiment and the smaller sample size may impact the results of the comparison. The regression analysis yielded values of 19.62 W/m^2K and 10.91 Ws/m^3K for U_0' and U_1' respectively.

Similar to Fig. 9, Fig. 11 also highlights the placement of HDF data in colour for three individual days from the total of 13 clear sky days collected. The behaviour of the red data can be explained by extremely high wind speeds cooling the module temperature to below 40 ℃. This causes the temperature gradient between the module and ambient air to be small, which causes $H/(T_{mod} - T_{amb})$ to be higher than the norm.

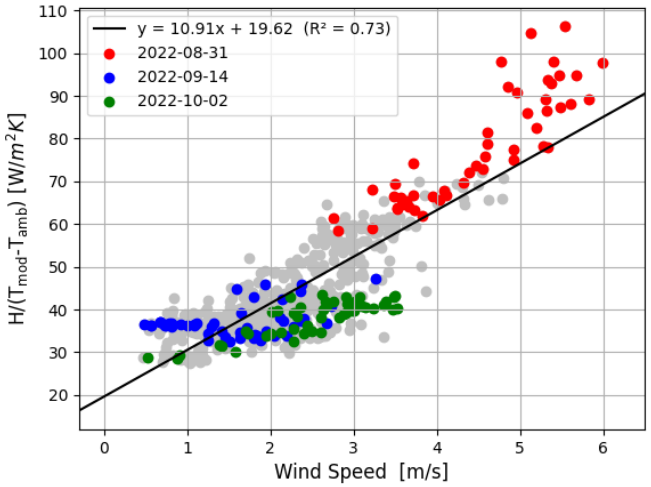

Fig. 11. FPV HDF curve

A comparison (not shown) of the conditions for the green and blue data indicates a steady, moderate wind speed for the day in green, with a lower, gradually increasing wind speed for the day in blue. Even though the wind speed for the green data is higher, a higher module-to-ambient temperature difference is observed. The blue data also shows a higher sensitivity to the lower wind speed compared to the effects of wind on the day in green. Here, it is again our postulation that wind direction plays a role.

The mean module temperature prediction for the FPV system has an RMSE of 3.72 ℃. The quality of the model's prediction versus the measured module temperature can be seen in Fig. 12.

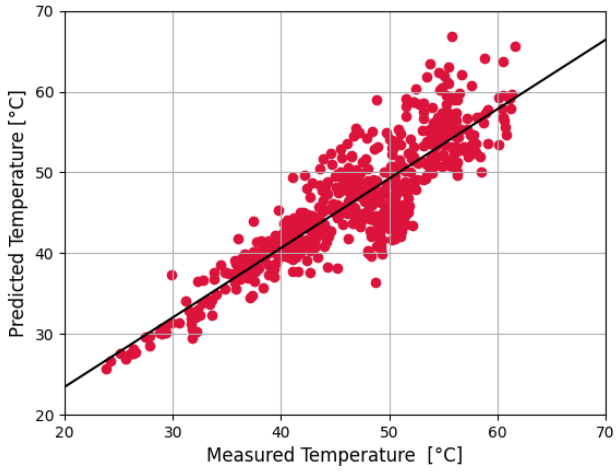

Fig. 12. FPV temperature prediction

The FPV HDFs found in this work compare relatively well to values reported in [8]. In [8], two distinct FPV systems were evaluated: one featured a closed float design and variable tilt panels ($U_0' = 24.4$ W/m^2K and $U_1' = 6.5$ Ws/m^3K with R^2 = 0.57), while the other employed a more open float array with a fixed panel tilt of 12° ($U_0' = 18.9$ W/m^2K and $U_1' = 8.9$ Ws/m^3K with R^2 = 0.58) in the Netherlands and Singapore

respectively. Data for each of these systems have been recorded on-site between 2017-2019. Additionally, two ground-based systems served as references near the two FPV sites: one in an open-rack configuration with a fixed panel tilt of 22° ($U_0' = 13.0$ W/m^2K and $U_1' = 5.4$ Ws/m^3K with R^2 = 0.52) and the other was a rooftop-mounted system ($U_0' = 18.9$ W/m^2K and $U_1' = 8.9$ Ws/m^3K with R^2 = 0.58) with a 10° panel tilt angle, located in the Netherlands and Singapore, respectively. The FPV system in Singapore is similar in configuration to the system considered in this work, except for the larger tilt angle at the Stellenbosch site (16°). Dörenkämper et al. [8] identified a significant influence of wind speed on the HDFs and concluded that higher wind speeds over open water, as well as the cooler air near water bodies, constitute the primary contributors to enhanced heat dissipation in FPV systems.

3.4. Discussion of PV Configuration Results

The U_1' value for the FPV system is higher than that of the open-rack configuration (10.91 Ws/m^3K compared to 9.90 Ws/m^3K). This is expected, due to higher wind spends carrying colder air [8] over FPV panels than for ground-based systems. When comparing the HDFs determined in this work, the FPV shows a lower U_0' but higher U_1' compared to the open-rack configuration. The higher wind dependent HDF (U_1') aligns with the findings of [8] and the that the water provides cooler ambient conditions around the installed modules. However, the lower FPV U_0' (19.62 W/m^2K compared to open-rack's 25.7 W/m^2K) value is somewhat unexpected and points to the need for FPV systems to be carefully configured if the full potential of lowering their operating temperatures are to be realized (as noted in [15]).

In this case, the FPV panels are less inclined than the open-rack system (16° compared to 31°). Lower tilt angles are typically chosen to mitigate wind loading on the system, but they may inadvertently impede natural convection heat dissipation. Furthermore, the presence of the float or the design thereof may further impact the ventilation of the back surfaces and, critically, prevents the back surface from being exposed to the cool water surface. The radiative heat loss from the back surface of the panels in the FPV case may thus be poorer than in the open-rack case.

It is important to note that the connection of the open-rack modules to a load resistor does not necessarily mean that these modules were operating at their maximum power point, in contrast to the FPV modules which were controlled to operate at maximum power. It is expected that the HDFs of the open-rack system would increase if they were to operate at their maximum power point, as the module temperatures should theoretically drop due to greater power evacuation from the modules while POA irradiance and ambient temperature would remain the same. The HDFs for the open-rack installation in this study are therefore likely to be relatively conservative.

3.5. Single Day Direct Comparison

To gain a deeper insight into the different thermal behaviours of the two PV configurations, a comparison is performed on a day with similar environmental conditions (POA irradiance, ambient temperature, and wind speed) as shown in Table 1.

Table 1. Environmental conditions for single day comparison

FPV - 2022/09/12			
	MIN	**MAX**	**MEAN**
Module Temp [°C]	28.9	46.5	40.7
Ambient Temp [°C]	14.5	18.4	16.6
$T_{mod} - T_{amb}$ [°C]	14.4	28.1	24.2
POA Irradiance [W/m^2]	637.5	983.3	885.3
Wind Speed [m/s]	0.80	2.65	1.39
$U_0' + U_1' \cdot v_w$ [W/m^2°C]	-	-	36.58
Open-rack - 2023/06/10			
Module Temp [°C]	29.3	42.6	38.2
Ambient Temp [°C]	14.6	17.7	16.2
$T_{mod} - T_{amb}$ [°C]	14.7	24.9	22.0
POA Irradiance [W/m^2]	598.1	892.4	813.7
Wind Speed [m/s]	1.23	2.48	1.78
$U_0' + U_1' \cdot v_w$ [W/m^2°C]	-	-	36.99

The data analysis reveals that the effective heat dissipation (represented by $H/(T_{mod} - T_{amb}) = U_0' + U_1' \cdot v_w$) for the two systems are virtually equivalent. This evaluation for a single day of similar conditions shows that, despite the lower averaged U_0' value obtained for the FPV system compared to the open-rack system, comparable heat dissipation from the FPV can be achieved.

4. Conclusion

The aim of the study was to compute and compare the HDFs according to Faiman's [1] thermal model for open-rack and FPV systems operating under similar environmental conditions. Experimental measurements were taken at an open-rack and FPV solar installation, both of which are located near Stellenbosch, South Africa. The measurement data for the two PV installations were filtered according to the method prescribed in [1].

The experimentally determined HDFs for the open-rack PV system align well with values reported in the literature [14], and the predicted temperature demonstrated an RMSE of 2.56 °C, indicating a reasonably accurate model. The value found for the wind-dependent HDF was consistent with values found in

literature [8] for FPV systems. However, the results of the FPV experiment revealed a lower U_0' than expected, with RMSE of 3.72 ℃ for the predicted temperatures. This suggests that, under low wind conditions, FPV systems dissipate heat less effectively than open-rack systems.

When comparing the thermal behaviour of the open-rack and FPV system on a day with similar environmental conditions, it was found that the FPV system's heat dissipation is comparable to that of the open-rack configuration.

The FPV system's relatively small tilt angle and float design were identified as potential contributing factors affecting the wind-independent heat dissipation, leading to higher-than-expected module temperatures, on average, compared to the open-rack configuration. This idea is further reinforced with the varying HDFs found in literature [8] for different FPV system designs. The floats used can affect the view factor the back of the FPV module experiences when radiating heat to the water.

In conclusion, the study highlights the importance of considering various design elements in FPV systems to optimize heat dissipation and module performance. By understanding the impact of tilt angle, float design, and module positioning on heat dissipation, researchers and designers can better enhance the thermal behaviour of FPV systems, maximizing their energy efficiency and overall performance.

Acknowledgements

The author would like to thank Scatec for providing the funding required to conduct this research and IFE for providing the necessary FPV data.

References

[1] D. Faiman, 'Assessing the outdoor operating temperature of photovoltaic modules', Progress in Photovoltaics: Research and Applications, vol. 16, pp. 307–315, Feb 2008.

[2] E. Barykina and A. Hammer, 'Modeling of photovoltaic module temperature using Faiman model: Sensitivity analysis for different climates', Solar Energy, vol. 146, pp. 401–416, 2017.

[3] Koehl, M., Heck, M., Wiesmeier, S., and Wirth, J., 'Modeling of the nominal operating cell temperature based on outdoor weathering', Solar Energy Materials & Solar Cells, vol. 95, pp. 1638-1646, 2011

[4] K. K. Agrawal, S. K. Jha, R. K. Mittal, and S. Vashishtha, 'Assessment of floating solar PV (FSPV) potential and water conservation: Case study on Rajghat Dam in Uttar Pradesh, India', Energy for Sustainable Development, vol. 66, pp. 287–295, Jan 2022.

[5] World Bank Group, *Where Sun Meets Water: Floating Solar Market Report—Executive Summary*, 2018, [Online]. Available:https://documents.worldbank.org/en/publication/documents-reports/documentdetail/579941540407455831.

[6] A. M. K. L. Abeykoon, G. M. L. P. Aponsu, H. M. B. I. Gunathilaka, and H. A. V. Nadeera, 'Effect of temperature on the photovoltaic characteristics of polycrystalline silicon solar cells at hambantota solar power plant', Solar Asia 2018 Int. Conf. National Institute of Fundamental Studies, Kandy, Sri Lanka, Jan 2018.

[7] D. Lindholm, T. Kjeldstad, J. Selj, E. S. Marstein, and H. G. Fjaer, 'Heat loss coeffients computed', Progress in Photovoltaics: Research and Applications, vol 29, pp. 1262-1273, July 2021.

[8] M. Dörenkämper, A. Wahed, A. Kumar, M. de Jong, J. Kroon, and T. Reindl, 'The cooling effect of floating PV in two different climate zones: A comparison of field test data from the Netherlands and Singapore', Solar Energy, vol. 219, pp. 15–23, May 2021.

[9] Weather Spark, *Average Weather in Cape Town, South Africa, Year Round*, 2019. [Online]. Available:https://weatherspark.com/y/82961/Average-Weather-in-Cape-Town-South-Africa-Year-Round

[10] A. Rix, K. Kritzinger, I. Meyer, and J.L. van Niekerk, "Potential for distributed solar photovoltaic systems in the Western Cape Province," Centre for Reneweable and Sustainable Energy Studies, 2015. [Online]. Available: https://www.crses.sun.ac.za/files/research/publications/technical-reports/WCG%20PV%20Report%20Final%5B1%5D.pdf

[11] Photovoltaic (PV) module performance testing and energy rating – Part 2: Spectral responsivity, incidence angle and module operating temperature measurements, IEC 61853-2 International Standard, Edition 1.0, Aug 2016.

[12] H. C. Hottel, A. Willier, 'Evaluation of Flat Plate Collector Performance'. Transactions of the Conference on the Use of Solar Energy, vol. 2, Part 1, University Of Arizona Press, pp. 74, 1958.

[13] R. W. Bliss, 'The Derivations of Several "Plate-Efficiency Factors" Useful in the Design of Flat-Plate Solar Heat Collectors', Solar Energy, vol. 3, pp. 55, 1959.

[14] M. Owen, J. Pretorius, B. Buitendag, and C. Nel, 'Heat dissipation factors for building-attached PV modules', International Heat Transfer Conference, Cape Town, South Africa, IHTC-17, ID-416, 2023.

[15] D. Lindholm, J. Selj, T. Kjeldstad, H. Fjær, and V. Nysted, 'CFD modelling to derive U-values for floating PV technologies with large water footprint', Solar Energy, vol. 238, pp. 238–247, May 2022.